Characteristics of polypropylene biocomposites: effect of chemical treatment to produce cellulose microfiber

Jaegwan Moon
Moorim P&P Co., Ltd
Jong Hoon Lee
Moorim P&P Co., Ltd
Kiseob Gwak
Moorim P&P Co., Ltd
Wanhee Im (iwh1009@moorim.co.kr)
Moorim P&P Co., Ltd https://orcid.org/0000-0001-7569-2038

Research Article

Keywords: Biocomposite, Cellulose microfiber, Chemical treatment, Reinforcement

Posted Date: April 28th, 2022

DOI: https://doi.org/10.21203/rs.3.rs-1535753/v1

Abstract

In this study, cellulose microfibers were prepared by sulfuric acid hydrolysis, glyoxal crosslinking and acetylation followed by air classifying mill, and their properties including chemical structure, particle size, appearance and crystallinity were investigated. The effect of cellulose microfibers properties on characteristics of polypropylene (PP) biocomposite, such as physical, thermal and mechanical properties, was also examined. The glyoxal crosslinking enhanced the brittleness of pulp fiber, resulting in smallest particle size of microfiber and thus less entanglement in the polymer matrix. When cellulose microfibers were incorporated into PP, the crystallinity of biocomposite decreased, irrespective of microfiber type due to interference crystallization during crystal growth. Additionally, glyoxal crosslinked cellulose microfiber decreased the crystallization temperature of biocomposite, which is different from the other types of cellulose microfiber. The good dispersibility and brittleness of glyoxal crosslinked microfiber contributed to enhanced mechanical properties of biocomposite compared to the other microfiber added biocomposites.

Introduction

Plastic is indispensable and essential to modern civilized society because it has excellent properties and low price compared to other materials (Andrady et al. 2009). Thanks to these advantages, a wide range of applications, such as packaging materials, digital devices, and medical equipment, are made from plastics. However, the use of plastic has led to various environmental problem. During its manufacture, plastic emits greenhouse gases that causes global warming and leaks endocrine disruptors when incised or buried. In addition, plastics flowed into the sea are threatening the ecosystem because it has been poorly biodegraded in nature (Lechner et al. 2014; Zarfl and Matthies. 2010). Human health is threatened by such plastic problems. Therefore, more and more consumers are interested in eco-friendly products, and countries are imposing harsh regulations on the use of plastic (Li and Zhao. 2017).

For this reason, considerable interest has been generated for developing and using eco-friendly biocomposite products. Biocomposite is the combination of natural fibers and polymer matrix (Ramamoorthy et al. 2015). Generally, various types of cellulose fibers such as wood fiber, kenaf, cotton, flax, hemp, jute and sisal have been used as reinforcement or fillers for biocomposite because of their biodegradable, inexpensive and renewable advantages (Alemdar and Sain. 2008). The mechanical properties of biocomposite are influenced by filler and matrix properties. The high strength and stiffness characteristics of pulp fibers could improve the strength of the biocomposite, which has been confirmed in several studies (Xie et al. 2010; Thakur and Thakur. 2014; Trache et al. 2016).

Among various types of cellulose-based fibers, wood fibers are manufactured in large quantities in pulping and papermaking processes. Thus, stable supply is possible, and the price is lower than that of non-wood or mineral fibers. Numerous studies that use wood pulp as reinforcement for biocomposites have been reported. For example, Peltola et al (2014) investigated the use of bleached soft wood kraft pulp to produce PP and polylactic acid (PLA) composite and found that the tensile strength and modulus

of biocomposite were improved significantly because of well-dispersed fibers in the polymer matrix. Besides, the addition of wood pulp reinforcement in the polymer matrix increases the degradation temperature and crystalline degree (López et al. 2012).

Although wood pulp is a suitable candidate for filler of biocomposite, there are challenges to overcome. Wood pulp has some drawbacks such as fluffy nature, low bulk density, high moisture absorption and incompatibility with most polymer matrix, etc. Notably, fluffy nature not only makes it difficult to feed raw materials into the extruder but also increase the transportation costs (Mahdavi et al. 2010). The fluffy nature of the pulp could be solved by manufacturing cellulose microfiber. Diverse manufacturing process to obtain cellulose microfiber exist, such as dry milling, chemical pretreatment and mixing of these technics. Acid hydrolysis is commonly used to produce cellulose microfiber like microcrystalline cellulose (MCC) on the industrial scale. However, the production process is not environmentally friendly because of the high concentration of sulfuric acid used in the manufacturing process (Araki et al. 1998). The use of high concentration sulfuric acid consumes a large amount of water for neutralization and generates high chemical oxygen demand (COD) of wastewater. Diverse chemical treatment methods had been studied for environmentally friendly production of cellulose microfiber. However, the effect of cellulose microfiber characteristics prepared by different chemical treatments on the performance of biocomposite has not been studied in detail.

In this study, the influence of chemical treatments on cellulose microfiber characteristics, such as morphology, chemical structure, crystallinity and so on, were investigated. Sulfuric acid hydrolysis, glyoxal crosslinking and acetylation were conducted to produce chemically treated cellulose microfiber. Polypropylene (PP) was selected as the matrix because it has easy processability, low price and high thermal stability. The biocomposites were produced by mixing cellulose microfiber, PP and compatibilizer at a ratio of 30%, 67% and 3%, respectively. In addition, the effect of microfiber types on physical, thermal and mechanical properties of biocomposites was also examined.

Materials And Methods

Materials

To prepare cellulose microfiber, hardwood bleached eucalyptus kraft pulp supplied by Moorim P&P, Korea, was used as a raw material. The pulp fiber consisted of 79.4 ± 0.6% cellulose, 18.8 ± 0.2% hemicellulose, and small amounts of lignin and ash, which was measured in accordance with the TAPPI method (T203 om-93). Sulfuric acid (OCI, extra pure grade), glyoxal, and acetic anhydride (Daejung Chemicals & Metals Co., Ltd, extra pure grade) were used as chemical reagents, and polypropylene (PP, Korea Petrochemical Ind. Co., Ltd, CB5230) was used as the polymer matrix. Additionally, maleic anhydride-grafted polypropylene (MAPP, IruChem Co., Ltd, IRUBOND 100) was used as a compatibilizer.

Preparation of cellulose microfiber

Three types of cellulose microfiber were prepared by different chemical treatments including sulfuric acid hydrolysis (S-Cellulose), glyoxal crosslinking (G-Cellulose) and acetylation (A-Cellulose). To prepare S-Cellulose, 300 g of pulp fiber was impregnated in 3 L of sulfuric acid diluted with deionized water to 10%, which was carried out under mild stirring condition for 1 hour at 95°C. After hydrolysis, reacted pulp fiber was washed with deionized water until its pH reached 7 ± 0.5 and the conductivity became lower than 30 μS/cm, followed by drying at 80°C for 24 hours.

In case of glyoxal crosslinking to prepare G-Cellulose, the reaction was conducted according to the methods described by Korpela and Orelma (2020). Briefly, 300 g of pulp fiber was immersed in 4% of glyoxal aqueous solution for 1 hour under liquid ratio of 1:5 solid-liquid ratio, and then cured in an oven at 110°C for 5 hours. A-Cellulose was prepared by acetylation with solvent-free method (Olaru et al. 2011). The pulp fiber was transferred to a polyethylene bag, followed by the addition of acetic anhydride under liquid ratio of 1:5 solid-liquid ratio. Next, 3 g of 95 wt% sulfuric acid was added as catalyst of the reaction. The acetylation was carried out at 40°C for 12 hours. After reaction, the obtained microfiber was also thoroughly washed using deionized water until the pH and conductively reached at desired conditions, and dried at 80°C for 24 hours. All dried pulp fiber was pulverized using an air classifying mill (ACM-300, KMTECH Co., Ltd., South Korea) at 5500 rpm, and sieved using a classifier (AS300, Retsch, Haan, Germany) equipped with 80 mesh screen. The cellulose microfiber accepted from the screen was stored in an oven at 80°C to prevent moisture adsorption.

Fabrication of biocomposite

The cellulose microfiber/PP biocomposite was extruded using twin screw extruder (BA-11, BAUTek, South Korea), which includes six consecutive heating zones. The temperatures of the six heating zone were set at 160°C, 170°C, 180°C, 190°C, 190°C, 190°C, respectively. The screw rotation speed of the extruder was fixed at 100 rpm, and corresponding production rate was 5g/min. Cellulose microfiber, PP and MAPP was mixed at a ratio of 30:67:3 to prepare biocomposites. The extruded biocomposite strands were cooled with a fan and cut intopellets with a pelletizer. The standard test samples were manufactured using an injection molder (BAUTek, BA 915a, South Korea) at a barrel temperature of 190°C. The biocomposites were classified as S-Composite, G-Composite, A-Composite depending on microfiber types

Characterization of cellulose microfibers

The presence of functional group in cellulose microfiber was characterized by Fourier-transformed infrared spectra analysis (FT-IR, 3100 FT-IR, Agilent Technologies Inc, USA). The attenuated total reflectance method was used, and all spectra were investigated in the wave number range from 600 to 4000 cm^{-1}. Particle size of cellulose microfibers was calculated by laser diffraction using a particle size analyzer (PSA 1190, Anton Paar GmbH, Austria). The morphologies of three types of cellulose microfiber were analyzed by scanning electron microscope observations (SEM, EVO MA10, ZEISS, Germany) at high vacuum condition and accelerating voltage of 20 kV. Before the observations, each sample was coated using ion coater for 120 seconds operating in the high vacuum condition with voltage of 20 kV. The crystallinity of the cellulose microfibers was analyzed using an X-ray diffractometer with a Cu Kα X-ray

source (XRD, D8 Advance, Bruker, Germany) set at 3 to 40 degrees with a scanning speed of 0.5 sec/step. The crystallinity index was estimated from the diffraction patterns according to the Segal method, as shown in Eq. (1).

Crystallinity (%) = $((I_{200} - I_{AM}))/I_{200)} \times 100$ (1)

Where I_{200} is the intensity of the 200 peak at 2θ = 22.7°, and I_{AM} is the minimum intensity between the 200 and 110 peaks at 2θ = 18°.

Physical properties of biocomposites

The density of specimens was investigated based on ASTM D792-13 with high accuracy scale and density determination kit (ML-DNY-43, METTLER TOLEDO, Canada) in distilled water. Measurement was repeated for three times and the average value was calculated. The melting flow index (MFI) of biocomposite was measured with MFI 452 (Wance, China) according to ASTM 1238-10. The MFI was analyzed using an applied load of 2.16 kg at 230°C. Three replicate measurements were undertaken for each sample. To determine water absorption of specimens, water uptake of sample was assessed in accordance with ASTM D570-98. Specimens were dried in an oven at 60°C for 24 hours and cooled in a desiccator. The weighted dry sample was immersed in water at 23°C for 24 hours. After immersion, the samples were wiped with a cloth to remove of water on surface and weighed immediately. Water absorption rate was calculated by the following Eq. (2).

Water absorption rate (%) = $((W_w - D_w) / D_w) \times 100$ (2)

where W_w is wet weight (g), D_w is dry weight (g).

Biocomposites films were prepared for dispersibility evaluation of cellulose microfibers in the polymer matrix. To prepare films, 5g of composite pallets were put into a hot press and pressed for 1 minute at 190°C with 30 bar pressure. The films were scanned at 2,400 dpi by a scanner. After that, the scanned image was cut into 3 × 3 cm size and converted to a binary image. Aggregate area ratio was evaluated from the binary image using an Image-J software.

Mechanical properties of biocomposites

Tensile test was conducted by standard method in accordance with ASTM D 638-03. Dumbbell shaped specimens were made, and tensile test was carried out using universal testing machine (AG-X-10kNX, SHIMADZU, Japan) at a load cell of 10 kN. The test gauge length and crosshead speed were fixed at 25 mm and 10 mm/min, respectively. Flexural strength was also measured according to ASTM D790-03 using same testing machine at 1.28 mm/min crosshead speed. All mechanical test was carried out at 25 ± 3°C and 50 ± 5% RH.

Results And Discussion

Characteristics of cellulose microfibers

To analyze the chemical structure of the cellulose microfibers prepared by chemical treatment, the FT-IR spectroscopic measurement was conducted, and results are shown in Fig. 1. The peak at 894 cm^{-1}, expressing C-O-C bond of β-glycosidic linkage, was observed in all sample irrespective of the type of chemical treatment (Oh et al. 2005). These results indicate that the chemical treatment used in this study did not decompose the β-glycosidic linkage of cellulose. The FT-IR spectrum of S-Cellulose microfiber showed the similar trend to the untreated pulp. This can be explained by the fact that the molecular structures of cellulose remain unchanged during sulfuric acid hydrolysis, which is consistent with previous studies (Tang et al. 2014; Chen et al. 2011). In case of G-Cellulose, the band intensity at approximately 3,300 cm^{-1} decreased, which related to the stretching vibration of O-H groups (Yang et al. 2011). This was a possible consequence of reaction between glyoxal and cellulose hydroxyl groups (Korpela and Orelma. 2020). When non-crosslinked glyoxal presented in cellulose fiber, it can be detected at 1735 cm^{-1} in FT-IR spectrum (Korpela and Orelma, 2020). However, there are no peak at around 1735 cm^{-1}, suggesting that complete crosslinking between cellulose and glyoxal was achieved. In case of A-Cellulose, three new peaks associated with acetylation appeared in FT-IR spectrum. The peak at 1750 cm^{-1} was originated from the carbonyl C = O stretching, and the peaks at 1368 cm^{-1} and 1230 cm^{-1} were originated from C-H bond bending in -O(C = O)-CH_3 and C-O stretching of acetyl group, respectively (Olaru et al. 2011). In addition, it was confirmed that the band disappeared at approximately 3,300 cm^{-1} by acetylation.

Figure 2 shows the appearance of cellulose microfibers prepared by different chemical treatments. As shown in Fig. 2, the length of cellulose microfibers significantly decreased after reaction compared to untreated pulp, regardless of treatment types. The mean size calculated by laser diffraction for untreated pulp, S-Cellulose, G-Cellulose, A-Cellulose microfiber were 54.6 μm, 23.1 μm, 21.1 μm, 41.4 μm, respectively. These size differences of cellulose microfibers can be easily confirmed by SEM image (Fig. 3). Although the same mechanical intensity was applied to prepare cellulose microfiber, the chemical reactions gave different morphological properties of cellulose microfiber. In particular, S-Cellulose microfiber had smaller particle size and spherical shape. This difference was likely attributed to sulfuric acid hydrolysis, which decreased the degree of polymerization of pulp and led to easier pulverization (He et al. 2018). It can be observed that the ends of G-Cellulose microfiber become broken by mechanical treatment, attributing that glyoxal crosslinking reaction increases the brittleness of pulp fiber. This is consistent with the result by Korpela and Orelma (2020). The pulp fiber treated by acetylation cannot be easily pulverized in longitudinal direction and generated entangled nature of microfiber. Lee and Mani (2017) reported that the aspect ratio of microfibers significantly affected their entanglement.

Figure 4 shows the results of XRD analysis. All cellulose microfiber exhibited typical diffraction peak profile of cellulose I (Tao et al. 2019). Sulfuric acid hydrolysis increased the crystallinity of cellulose microfiber, while glyoxal crosslinking and acetylation decreased the crystallinity of cellulose microfiber. The aldehyde group of glyoxal and the acetyl group of acetic anhydride reacted with the hydroxyl group

of cellulose during the chemical treatment (Shuzhen et al. 2018; Li et al. 2009). Thus, the inter- and intra-molecular hydrogen bonds in cellulose might be decreased, resulting in lower crystallinity of cellulose compared to untreated pulp microfiber (Nabili et al. 2017).

Characteristics of biocomposites

The density and MFI of biocomposites are presented in Table 1. The density of the three biocomposite were very similar, ranging from 0.99 g/m^3 to 1.01 g/m^3, while the density of neat PP was 0.9 g/m^3. This result indicates that the addition of cellulose microfiber in the polymer matrix increased the density of biocomposite, irrespective of treatment type, because the density of cellulose is 1.5 g/m^3 (Svagan et al. 2008, Varanasi et al. 2013).

In addition, the MFI of biocomposites was significantly affected by the cellulose microfiber types (Table 1). The MFI determines the flowability of a polymer material (Irwanto et al. 2019), and it indirectly reflects the viscosity and molecular weight of composites (Minoshima et al. 1980). Generally, higher density leads to higher viscosity and lower flowability. In this study, the addition of cellulose microfiber decreased the MFI, regardless of chemical treatment types. The reason for the decrease in MFI is that the PP polymer melts and becomes a molten state like liquid, while cellulose microfiber remains solid state during the measurement. Thus, the cellulose microfiber embedded in polymer matrix may cause hindered flow (Indrajati et al. 2020). Among the three biocomposites, the A-Cellulose microfiber-added biocomposite exhibited the lowest MFI compared with the other two biocomposites. This result can be attributed to the fact that higher length of microfiber tends to decrease the MFI of polymer due to longer additives would disturb the flow (Kumari et al. 2007).

Biocomposites often display high sensitivity to moisture due to hydrophilic nature of cellulose. This characteristic can decrease the dimensional stability, mechanical property and durability of biocomposites (Huang et al. 2020). The amount of water absorption of biocomposite samples is also presented in Table 1. Neat PP exhibited extremely low water absorption rate of 0.08%. Among all biocomposites, the A-Composite, which was extruded with acetylated cellulose microfiber, presented the lowest water absorption rate because the hydrophobicity of A-Cellulose microfiber increased by acetylation.

Table 1
Characteristics of biocomposites

	Neat PP	S-Composite	G-Composite	A-Composite
Density, g/m^3	0.90 ± 0.01	0.99 ± 0.02	1.01 ± 0.02	0.99 ± 0.01
Melt flow index, g/10 min	31.6 ± 0.8	17.2 ± 1.2	17.3 ± 0.9	5.2 ± 1.0
Water absorption rate, %	0.08 ± 0.04	1.49 ± 0.46	1.61 ± 0.32	0.93 ± 0.23

Figure 5 depicts the dispersibility of cellulose microfibers in the polymer matrix. The aggregated cellulose microfibers can be confirmed as white dots in the binary image. As shown clearly, the appearance of aggregated A-Cellulose microfibers can be seen all over the image of its film, which means that A-Cellulose microfiber had inferior dispersibility than S- and G-Cellulose microfibers. The aggregate area ratio of S-, G-, and A-Composite was 1.6%, 1.9%, and 12.4%, respectively. Although acetylation has been conducted to enhance the compatibility between natural fiber and polymer (Tingaut et al. 2010), the length of microfiber most probably affected the dispersibility of microfiber in polymer matrix.

Thermal properties of biocomposites

DSC is widely used to determine the thermal parameters and crystallization mechanism of polymer system (Patel et al. 2013). The effect of the cellulose microfibers on the thermal properties of biocomposite is summarized in Table 2 and presented in Fig. 6. The heating run was measured to obtain the melting temperature and melting enthalpy. As shown in Table 1, the addition of cellulose microfibers decreased the crystallinity (χ_c) of biocomposite compared with neat PP. It can be explained that the amount of PP that can be crystallized decreased due to the interference of cellulose microfibers with the crystallization during the crystal growth (Asumani et al. 2012).

All the samples exhibited wide melting endotherm around 166°C (Fig. 6(a)), suggesting that only the α (monoclinic) crystalline polymorph of PP was present (Santis et al. 2006). In general, cellulose fiber can act as a nucleating agent for PP matrix during the nucleation stage, resulting in an increase in the crystallization temperature (T_c). The nucleating effects of cellulose fiber is enhanced by MAPP, which causes the strong interaction of cellulose fiber with PP matrix by covalent bonds with hydroxyl groups (Huang et al. 2018). However, there was no increasing crystallization temperature of S- and A-Composite in this study. Different from S- and A-Composite, the crystallization temperature of G-Composite shifted to approximately 122°C. This is because the hydroxyl groups of cellulose crosslinked with glyoxal and formed covalent bridges. Therefore, its ability of forming covalent bonds between PP and cellulose microfibers relatively decreased than other two types of cellulose microfibers. The decrease in the crystallization temperature contributes to the shortened the manufacturing process (Kuciel et al. 2014).

Table 2
DSC parameters of biocomposites

Sample	T_c, °C	ΔH_c, J/g	T_m, °C	ΔH_m, J/g	χ_c, %
Neat PP	130.3	71.4	166.9	67.7	32.4
S-Composite	130.3	65.4	166.9	69.5	22.3
G-Composite	122.7	61.5	165.3	60.1	19.3
A-Composite	130.1	60.6	167.0	52.9	17.0

Mechanical properties of biocomposites

Mechanical properties of biocomposite including tensile and flexural strength were evaluated as shown in Table 3. The addition of S-Cellulose microfiber did not impose a significant effect on the tensile properties of biocomposite. On the contrary, G- and A-Cellulose microfiber affected the tensile properties of biocomposites. The highest tensile properties of biocomposite were achieved with G-Cellulose microfiber. This was attributed to the good dispersibility of G-Cellulose microfiber, as shown in Fig. 5. The increased brittleness of cellulose by cross-linking is another possible reason for an increase in tensile properties (Korpela and Orelma, 2020). In the case of A-Composite, the addition of A-Cellulose microfiber decreased the tensile strength of composite by 21.9% compared to neat PP. Similar result has been reported by Luz et al (2008). The elongation at break of biocomposites significantly decreased due to very low elongation of cellulose microfibers irrespective of the chemical treatment (Sirviö et al. 2018). Flexural properties of biocomposite exhibited higher value than neat PP, regardless of the type of cellulose microfiber. This is because flexural properties rely on the stiffness of reinforcement (Bledzki et al. 2015; Karmarkar et al. 2007). The measured flexural properties increased in the order of G-, S-, A-Composite, same as tensile properties.

Table 3
Mechanical properties of biocomposites

		Neat PP	S-Composite	G-Composite	A-Composite
Tensile	Strength, MPa	30.8 ± 0.9	30.8 ± 0.3	40.3 ± 2.0	25.4 ± 0.8
	Modulus, MPa	1395.8 ± 103.2	1544.9 ± 152.6	1763.3 ± 120.4	1388.9 ± 66.2
	Elongation at break, %	230.2 ± 14.4	3.8 ± 0.7	8.6 ± 0.7	8.0 ± 0.3
Flexural	Strength, MPa	46.2 ± 1.4	52.4 ± 1.4	61.6 ± 1.3	45.8 ± 1.9
	Modulus, MPa	1395.8 ± 125.7	2824.7 ± 68.6	3428.3 ± 219.6	2274.1 ± 180.2

Conclusions

The influence of cellulose microfiber characteristics including chemical structure, morphological properties, crystallinity on the properties of PP biocomposites was investigated. Sulfuric acid hydrolyzed, glyoxal crosslinked and acetylated cellulose microfiber were prepared as a polymer reinforcement. The morphology of microfiber was significantly influenced by the chemical treatment types. Sulfuric acid hydrolyzed and glyoxal crosslinked pulp fiber can be easily pulverized to smaller size at the same mechanical treatment condition than acetylated pulp fiber, resulting in better dispersibility in the polymer matrix. The addition of cellulose microfiber decreased the crystallinity of biocomposite, regardless of microfiber type. This is because cellulose microfiber interference polymer crystallization during crystal

growth. In addition, G-Cellulose microfiber decreased the crystallization temperature of biocomposite due to the crosslinking between hydroxyl groups of cellulose and glyoxal. The overall mechanical strengths of biocomposite were improved by reinforcing effect of cellulose microfiber. Especially, the addition of G-Cellulose microfiber enhanced the mechanical properties than the other two types of microfibers due to its good dispersibility and brittleness.

Declarations

Acknowledgments

This study was carried out with the support of 'Forest Science & Technology Projects (Project No 2020214B10-2222-AC01) provided by Korea Forest Service.

References

1. Alemdar A, Sain M (2008) Biocomposites from wheat straw nanofibers: morphology, thermal and mechanical properties. Compos Sci Technol 68:557–565. https://doi.org/10.1016/j.compscitech.2007.05.044
2. Anthony LA, Mike AN (2009) Applications and societal benefits of plastics. Philos Trans R Soc B 364:1977–1984 https://doi.org/10.1098/rstb.2008.0304
3. Araki J, Wada M, Kuga S, Okano T (1998) Flow properties of microcrystalline cellulose suspension prepared by acid treatment of native cellulose. Colloids Surf A 142:75–82. https://doi.org/10.1016/S0927-7757(98)00404-X
4. Asumani OML, Reid RG, Paskaramoorthy R (2012) The effects of alkali–silane treatment on the tensile and flexural properties of short fibre nonwoven kenaf reinforced polypropylene composites. Compos Part A 43:1431–1440. https://doi.org/10.1016/j.compositesa.2012.04.007
5. Beg MDH, Pickering KL (2008) Mechanical performance of Kraft fibre reinforced polypropylene composites: Influence of fibre length, fibre beating and hygrothermal ageing. Compos Part A 39:1748–1755. https://doi.org/10.1016/j.compositesa.2008.08.003
6. Bledzki AK, Franciszczak P, Osman Z, Elbadawi M (2015) Polypropylene biocomposites reinforced with softwood, abaca, jute, and kenaf fibers. Ind Crops Prod 70:91–99. https://doi.org/10.1016/j.indcrop.2015.03.013
7. Chen W, Yu H, Liu Y (2011) Preparation of millimeter-long cellulose I nanofibers with diameters of 30–80 nm from bamboo fibers. Carbohydr Polym 86:453–461. https://doi.org/10.1016/j.carbpol.2011.04.061
8. He Q, Wang Q, Zhou H, Ren D, He Y, Cong H, Wu L (2018) Highly crystalline cellulose from brown seaweed Saccharina japonica: isolation, characterization and microcrystallization. Cellulose 25:5523–5533. https://doi.org/10.1007/s10570-018-1966-1

9. Huang CW, Yang TC, Hung KC, Xu JW, We JH (2018) The effect of maleated polypropylene on the non-Isothermal crystallization kinetics of wood fiber-reinforced polypropylene composites. Polymers 10:382. https://doi.org/10.3390/polym10040382
10. Huang L, We Q, Wang Q, Ou R, Wolcott M (2020) Solvent-free pulverization and surface fatty acylation of pulp fiber for property-enhanced cellulose/polypropylene composites. J Clean Prod 244:118811. https://doi.org/10.1016/j.jclepro.2019.118811
11. Indrajati IM, Dewi IR, Nurhajati DW (2020) Properties of microfibrillar cellulose filled thermoplastic natural rubber: morphology, mechanical properties, and melt flow index. Majalah Kulit Karet dan Plastik 36:89–100. https://doi.org/10.20543/mkkp.v36i2.6522
12. Irwanto D, Pidhatika B, Nurhajati DW, Harjanto S (2019) Mechanical properties and crystallinity of linier low density polyethylene based biocomposite film. Majalah Kulit Karet dan Plastik 35:93–98. https://doi.org/10.20543/mkkp.v35i2.5624
13. Karmarkar A, Chauhan SS, Modak JM, Chanda M (2007) Mechanical properties of wood–fiber reinforced polypropylene composites: effect of a novel compatibilizer with isocyanate functional group. Compos Part A 38:227–233. https://doi.org/10.1016/j.compositesa.2006.05.005
14. Korpela A, Orelma H (2020) Manufacture of fine cellulose powder from chemically crosslinked kraft pulp sheets using dry milling. Powder Technol 361:642–650. https://doi.org/10.1016/j.powtec.2019.11.064
15. Kuciel S, Jakubowska P, Kuźniar P (2014) A study on the mechanical properties and the influence of water uptake and temperature on biocomposites based on polyethylene from renewable sources. Compos Part B 64:72–77. https://doi.org/10.1016/j.compositesb.2014.03.026
16. Kumari R, Ito H, Takatani M, Uchiyama M, Okamoto T (2007) Fundamental studies on wood/cellulose–plastic composites: effects of composition and cellulose dimension on the properties of cellulose/PP composite. J Wood Sci 53:470–480 https://doi.org/10.1007/s10086-007-0889-5
17. Lechner A, Keckeis H, Lumesberger-Loisl F, Zens B, Krusch R, Tritthart M, Glas M, Schldermann E (2014) The Danube so colourful: a potpourri of plastic litter outnumbers fish larvae in Europe's second largest river. Environ Pollut 188:177–181. https://doi.org/10.1016/j.envpol.2014.02.006
18. Lee H, Mani S (2017) Mechanical pretreatment of cellulose pulp to produce cellulose nanofibrils using a dry grinding method. Ind Crops Prod 103:179–187. https://doi.org/10.1016/j.indcrop.2017.04.044
19. Li J, Fukuoka T, He Y, Uyama H, Kobayashi S, Inoue Y (2005) Thermal and crystallization behavior of hydrogen-bonded miscible blend of poly(3-hydroxybutyrate) and enzymatically polymerized polyphenol. J Appl Polym Sci 97:2439–2449. https://doi.org/10.1002/app.22004|
20. Li J, Zhang LP, Peng F, Bian J, Yuan TQ, Xu F, Sun RC (2009) Microwave-Assisted Solvent-Free Acetylation of Cellulose with Acetic Anhydride in the Presence of Iodine as a Catalyst. Molecules 14:3551–3566. https://doi.org/10.3390/molecules14093551

21. Li Z, Zhao F (2017) An analytical hierarchy process-based study on the factors affecting legislation on plastic bags in the USA. Waste Manage Res 35:795–809. https://doi.org/10.1177/0734242X17705725
22. López JP, Gironès J, Méndez JA, Mansouri NEE, Llop MF, Mutjé P, Vilaseca F (2012) Stone-ground wood pulp-reinforced polypropylene composites: water uptake and thermal properties. BioResources 7:5478–5487. https://doi.org/10.15376/biores.7.4.5478-5487
23. Luz SM, Tio JD, Rocha GJ, Gonçalves M, Del'Arco AR Jr AP (2008) Cellulose and cellulignin from sugarcane bagasse reinforced polypropylene composites: Effect of acetylation on mechanical and thermal properties. Compos Part A 39:1362–1369. https://doi.org/10.1016/j.compositesa.2008.04.014
24. Mahdavi S, Kermanian H, Varshoei A (2010) Comparison of mechanical properties of date palm fiber-polyethylene composite. BioResources 5:2391–2403
25. Minoshima W, White JL, Spruiell JE (1980) Experimental investigation of the influence of molecular weight distribution on the rheological properties of polypropylene. Polym Eng Sci 20:1166–1176. https://doi.org/10.1002/pen.760201710
26. Nabili A, Fattoum A, Brochier-Salon MC, Bras J, Elaloui E (2017) Synthesis of cellulose triacetate-I from microfibrillated date seeds cellulose (Phoenix dactylifera L.). Iran Polym J 26:137–147. https://doi.org/10.1007/s13726-017-0505-5
27. Oh SY, Yoo DI, Shin Y, Kim HC, Kim HY, Chung YS, Park WH, Youk JH (2005) Crystalline structure analysis of cellulose treated with sodium hydroxide and carbon dioxide by means of X-ray diffraction and FTIR spectroscopy. Carbohydr Res 340:2376–2391. https://doi.org/10.1016/j.carres.2005.08.007
28. Olaru N, Olaru L, Vasile C, Ander P (2011) Surface modified cellulose obtained by acetylation without solvents of bleached and unbleached kraft pulps. Polimery 56:834–840. https://doi.org/10.14314/polimery.2011.834
29. Patel AK, Bajpai R, Keller JM (2013) On the crystallinity of PVA/palm leaf biocomposite using DSC and XRD techniques. Microsyst Technol 20:41–49. https://doi.org/10.1007/s00542-013-1882-0
30. Peltola H, Pääkkönen E, Jetsu P, Heinemann S (2014) Wood based PLA and PP composites: Effect of fibre type and matrix polymer on fibre morphology, dispersion and composite properties. Compos Part A 61:13–22. https://doi.org/10.1016/j.compositesa.2014.02.002
31. Ramamoorthy SK, Skrifvars M, Persson A (2015) A review of natural fibers used in biocomposites: plant, animal and regenerated cellulose fiber. Polym Rev 55:107–162. https://doi.org/10.1080/15583724.2014.971124
32. Santis FD, Adamovsky S, Titomanliso G, Schick C (2006) Scanning nanocalorimetry at high cooling rate of isotactic polypropylene. Micromolecules 39:2562–2567. https://doi.org/10.1021/ma052525n
33. Shuzhen N, Liang J, Hui Z, Yongchao Z, Guigan F, Huining X, Hongqi D (2018) Enhancing hydrophobicity, strength and UV shielding capacity of starch film via novel co-cross-linking in neutral conditions. R Soc Open Sci 5:181206. https://doi.org/10.1098/rsos.181206

34. Sirviö JA, Visanko M, Ukkola J, Liimatainen H (2018) Effect of plasticizers on the mechanical and thermomechanical properties of cellulose-based biocomposite films. Ind Crops Prod 122:513–521. https://doi.org/10.1016/j.indcrop.2018.06.039
35. Svagan AJ, Azizi Samir MAS, Berglund LA (2008) Biomimetic foams of high mechanical performance based on nanostructured cell wall reinforced by native cellulose nanofibrils. Adv Mater 20:1263–1269. https://doi.org/10.1002/adma.200701215
36. Tang Y, Yang S, Zhang N, Zhang J (2014) Preparation and characterization of nanocrystalline cellulose via low-intensity ultrasonic-assisted sulfuric acid hydrolysis. Cellulose 21:335–346. https://doi.org/10.1007/s10570-013-0158-2
37. Tao P, Zhang Y, Wu Z, Liao X, Nie S (2019) Enzymatic pretreatment for cellulose nanofibrils isolation from bagasse pulp: transition of cellulose crystal structure. Carbohydr Polym 214:1–7. https://doi.org/10.1016/j.carbpol.2019.03.012
38. Thakur VK, Thakur MK (2014) Processing and characterization of natural cellulose fibers/thermoset polymer composites. Carbohydr Polym 109:102–117. https://doi.org/10.1016/j.carbpol.2014.03.039
39. Tingaut P, Zimmermann T, Lopez-Suevos F (2010) Synthesis and characterization of bionanocomposites with tunable properties from poly(lactic acid) and acetylated microfibrillated cellulose. Biomacromolecules 11:454–464. https://doi.org/10.1021/bm901186u
40. Trache D, Hussion MH, Chuin CTH, Sabar S, Nurul Fazita MR, Taiwo OFA, Hassan TM, Haafiz MKM (2016) Microcrystalline cellulose: Isolation, characterization and bio-composites application—A. Rev Int J Biol Macromol 93:789–804. https://doi.org/10.1016/j.ijbiomac.2016.09.056
41. Varanasi S, He R, Batchelor W (2013) Estimation of cellulose nanofibre aspect ratio from measurements of fibre suspension gel point. Cellulose 20:1885–1896. https://doi.org/10.1007/s10570-013-9972-9
42. Xie Y, Hill CAS, Xiao Z, Militz H, Mai C (2010) Silane coupling agents used for natural fiber/polymer composites: A review. Compos Part A 41:806–819. https://doi.org/10.1016/j.compositesa.2010.03.005
43. Yang Q, Pan X, Huang F, Li K (2011) Synthesis and characterization of cellulose fibers grafted with hyperbranched poly (3-methyl-3-oxetanemethanol). Cellulose 18:1611–1621. https://doi.org/10.1007/s10570-011-9587-y
44. Zarfl C, Matthies M (2010) Are marine plastic particles transport vectors for organic pollutants to the arctic? Mar Pollut Bull 60:1810–1814. https://doi.org/10.1016/j.marpolbul.2010.05.026

Figures

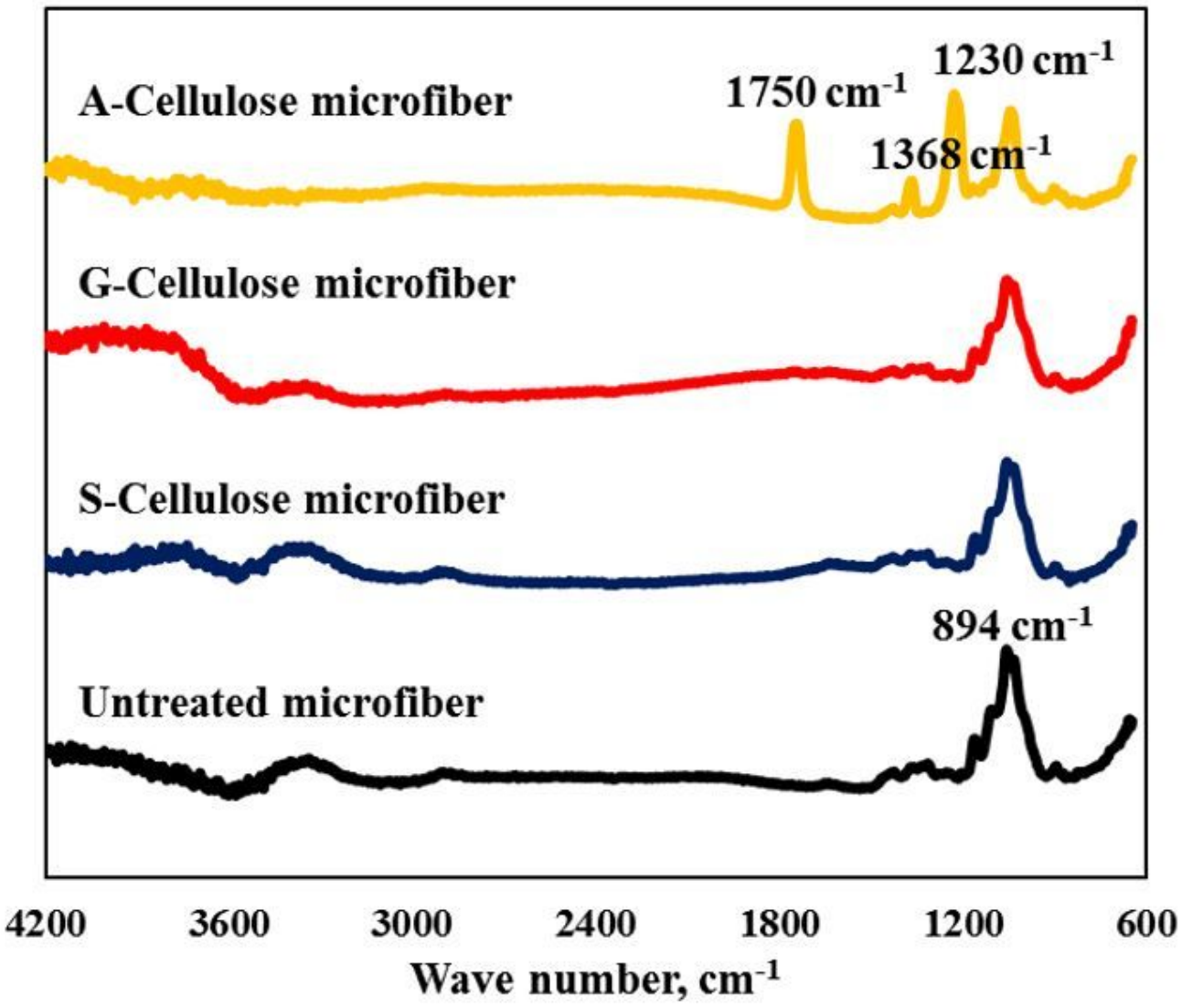

Figure 1

FT-IR spectra of cellulose microfibers

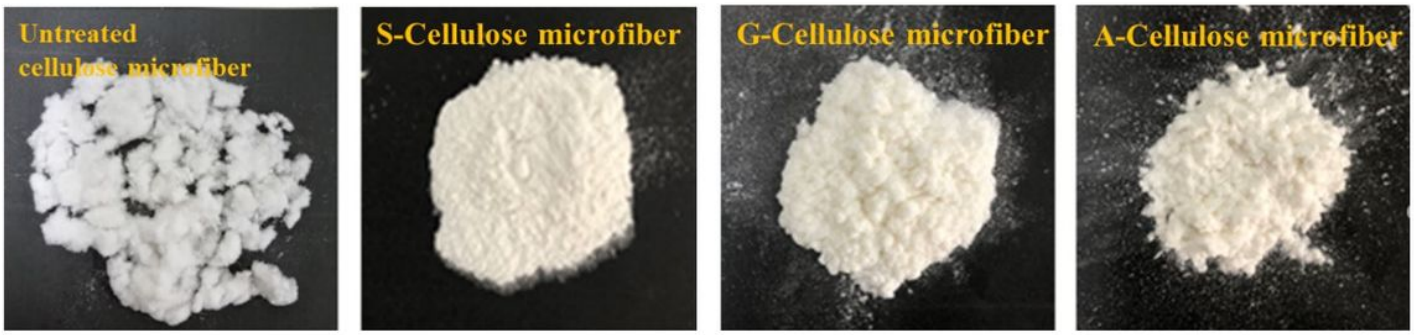

Figure 2

Appearance of cellulose microfibers prepared by different chemical treatments

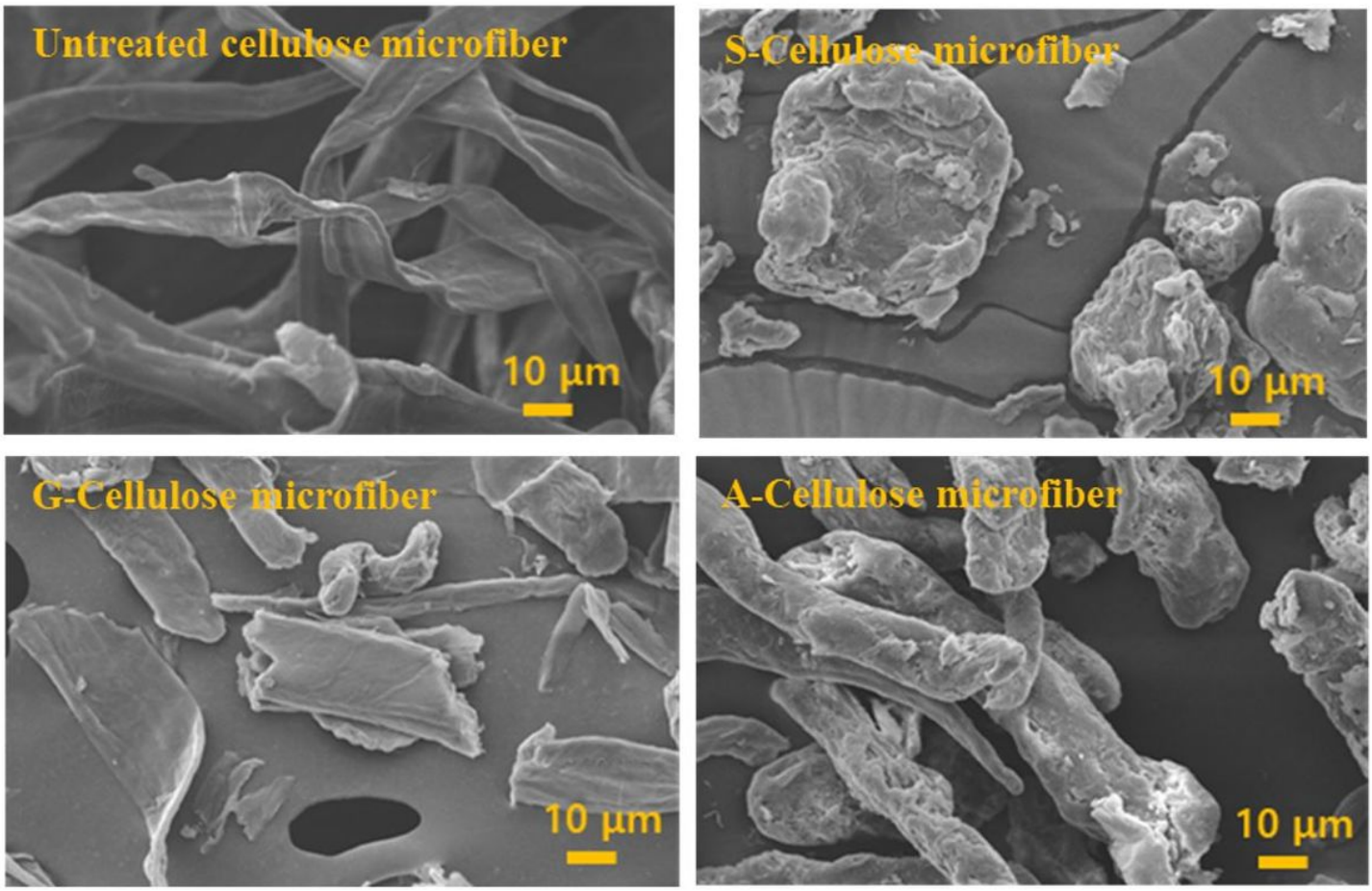

Figure 3

The morphological properties of cellulose microfibers

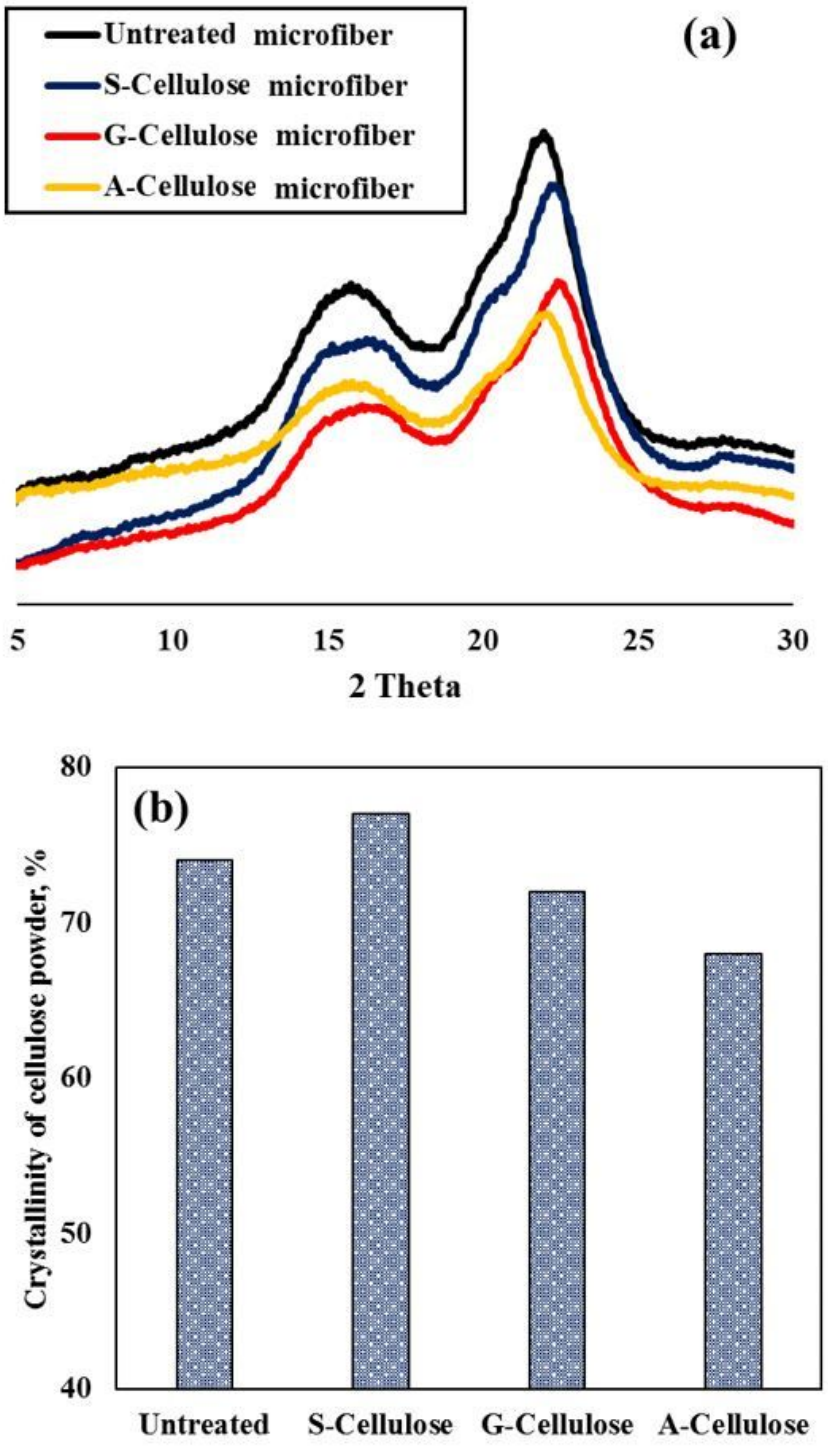

Figure 4

XRD pattern (a) and crystallinity (b) of cellulose microfibers

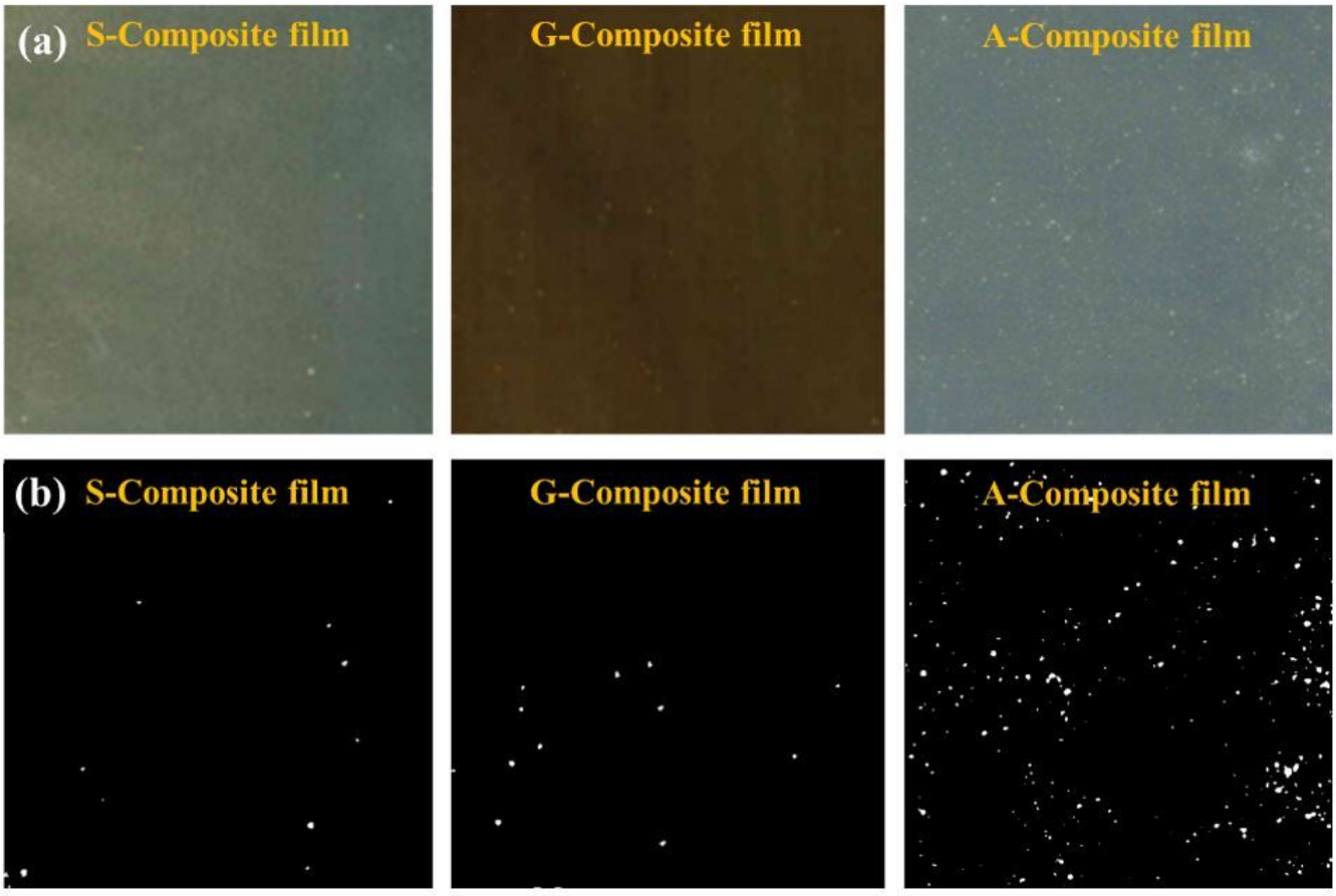

Figure 5

Dispersibility of cellulose microfiber in the polymer matrix: original image (a) and binary image (b)

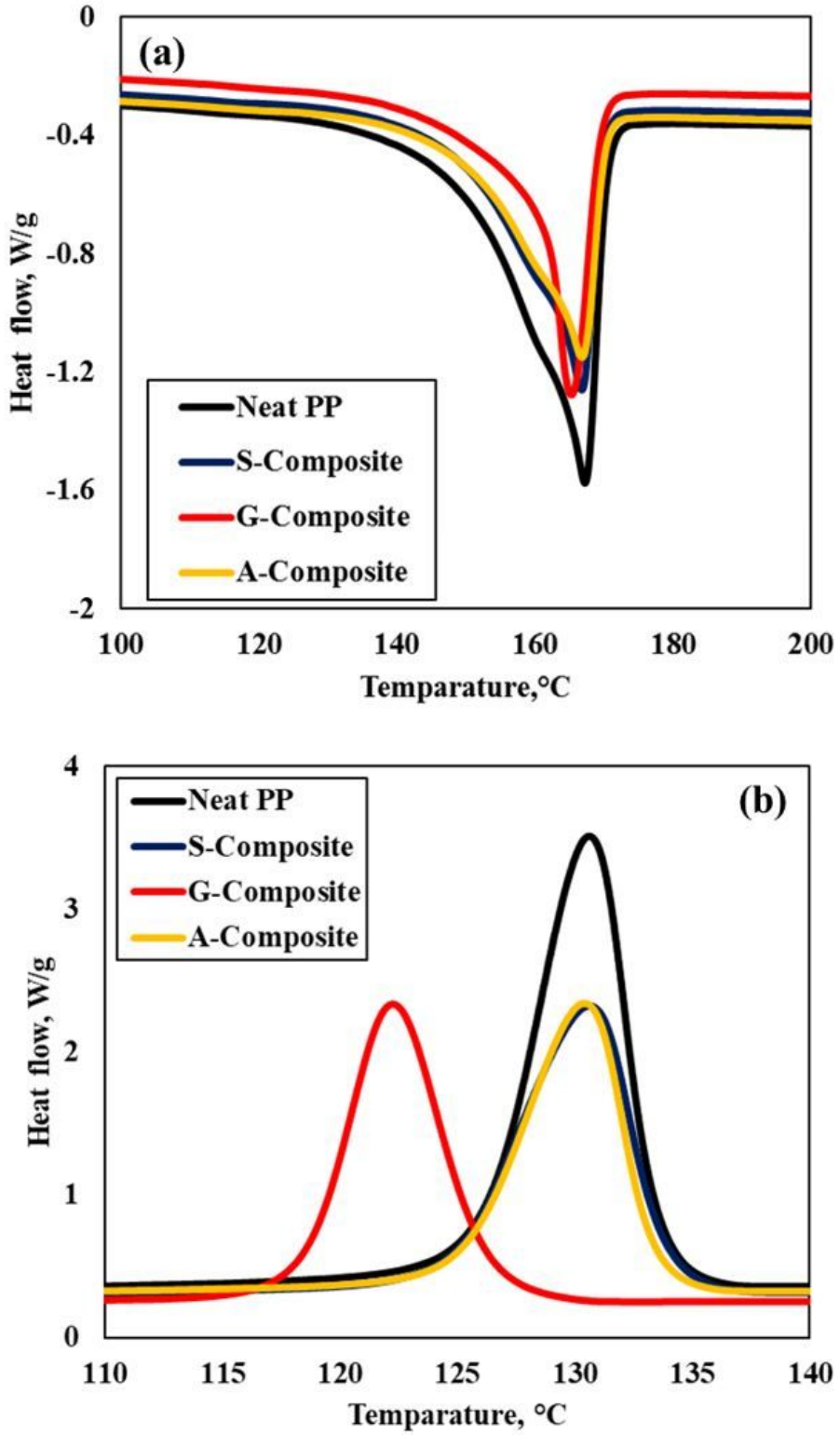

Figure 6

Melting (a) and crystallization temperature (b) of neat PP and biocomposite